Title

The evolutionary dynamics of local adaptations under genetic rescue is determined by mutational load and polygenicity

Journal

Journal of Heredity, 115(4)

ISSN

0022-1503

Authors

Zhang, Yulin

Stern, Aaron J

Nielsen, Rasmus

Publication Date

2024-07-10

DOI

10.1093/jhered/esad079

Peer reviewed

Journal of Heredity, 2024, **115**, 373–384
https://doi.org/10.1093/jhered/esad079
Advance access publication 26 December 2023
Original Article

Original Article

The evolutionary dynamics of local adaptations under genetic rescue is determined by mutational load and polygenicity

Yulin Zhang[1,2,*,†], **Aaron J. Stern**[2,*,†] **and Rasmus Nielsen**[3,4,5]

[1]School of Life Sciences, Sun Yat-sen University, Guangzhou, Guangdong, P.R. China,
[2]Center for Computational Biology, UC Berkeley, Berkeley, CA, United States,
[3]Department of Integrative Biology, UC Berkeley, Berkeley, CA, United States,
[4]Department of Statistics, UC Berkeley, Berkeley, CA, United States,
[5]Center for GeoGenetics, Globe Institute, University of Copenhagen, Copenhagen, Denmark

[†]These authors contributed equally.
[*]Corresponding authors: Center for Computational Biology, UC Berkeley, CA, United States, 94720. Email: zhangyulin9806@berkeley.edu (YZ); Center for Computational Biology, UC Berkeley, CA, United States, 94720. Email: ajstern@berkeley.edu (AJS), Department of Integrative Biology, UC Berkeley, CA, United States, 94720. Email: rasmus_nielsen@berkeley.edu (RN)

Corresponding Editor: Kirk Lohmueller

Abstract

Inbred populations often suffer from increased mutational load and reduced fitness due to lower efficacy of purifying selection in groups with small effective population sizes. Genetic rescue (GR) is a conservation tool that is studied and deployed with the aim of increasing the fitness of such inbred populations by assisted migration of individuals from closely related outbred populations. The success of GR depends on several factors—such as their demographic history and distribution of dominance effects of mutations—that may vary across populations. While we understand the impact of these factors on the dynamics of GR, their impact on local adaptations remains unclear. To this end, we conduct a population genetics simulation study to evaluate the impact of trait complexity (Mendelian vs. polygenic), dominance effects, and demographic history on the efficacy of GR. We find that the impact on local adaptations depends highly on the mutational load at the time of GR, which is in turn shaped dynamically by interactions between demographic history and dominance effects of deleterious variation. Over time local adaptations are generally restored post-GR, though in the short term they are often compromised in the process of purging deleterious variation. We also show that while local adaptations are almost always fully restored, the degree to which ancestral genetic variation affecting the trait is replaced by donor variation can vary drastically and is especially high for complex traits. Our results provide insights on the impact of GR on trait evolution and considerations for the practical implementation of GR.

Received June 27, 2023; Accepted December 22, 2023

Graphical Abstract

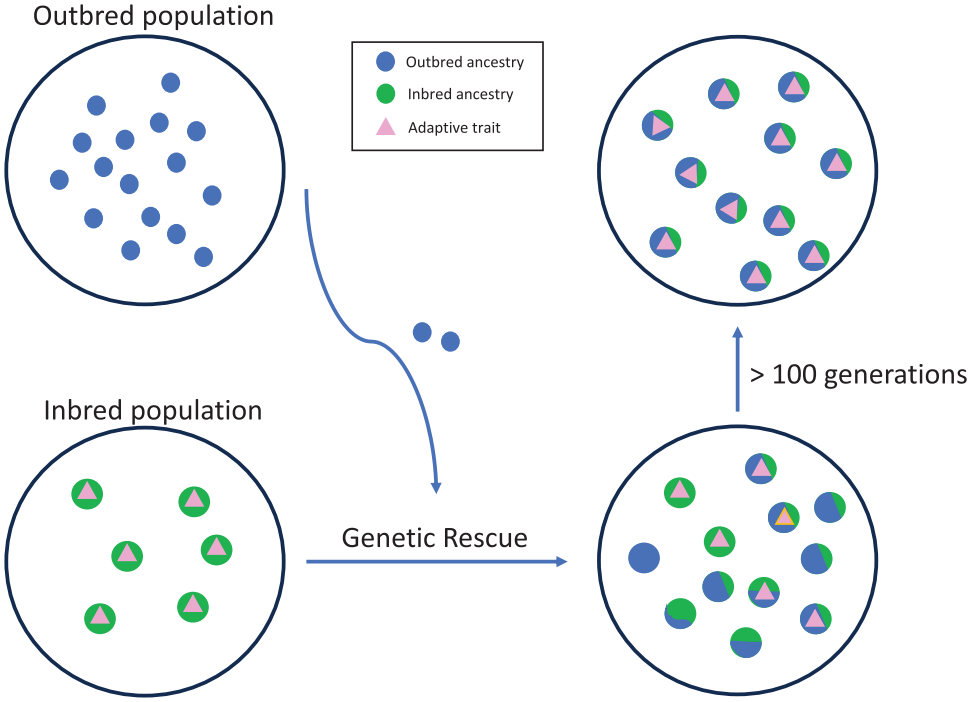

Key words: conservation genetics, demographic history, dominance, genetic rescue, local adaptations, mutational load, polygenic traits

Introduction

Genetic rescue (GR) is a strategy used in conservation biology that aims to increase the fitness of an endangered inbred (recipient) population by introducing genetic variation from another (donor) population. GR is accomplished by assisted migration of individuals from closely related, healthy populations to the imperiled inbred population. This process, by definition, leads to the replacement of local genetic variation in the recipient population from the donor population. Typically, only a small number of individuals are introduced in order to conserve local genetic variation (Whiteley et al. 2015).

The strategy has now been practiced on many highly inbred populations from different taxa, including the Florida panther (Johnson et al. 2010), African lions (Miller, et al. 2020), robins (Heber et al. 2012), guppies (Fitzpatrick et al. 2016), woodrats (Smyser et al. 2013), and adders (Madsen et al. 1999). In several cases, GR efficiently increased the absolute fitness of the inbred population and reduced inbreeding depression (Frankham 2015; Hedrick and Garciadorado 2016). A famous example is the introduction of mountain lions from Texas of the subspecies *Puma concolor stanleyana (P. c. stanleyana)* to the Florida *Puma concolor coryi (P. c. coryi)* population, which resulted in a 3-fold increase in the number of *P. c. coryi* within five years, coupled with increased survival rates and a doubling of heterozygosity in the recipient population (Johnson et al. 2010). Analytical and empirical studies indicate that the beneficial effect of GR can persist over multiple generations (Frankham 2016; Jørgensen et al. 2022). These findings underscore the potential of GR as a powerful conservation tool for increasing fitness in endangered inbred populations.

However, despite its promise, there is skepticism and caution towards the application of GR due to concerns about outbreeding depression and genetic homogenization (Rhymer and Simberloff 1996; Gharrett et al. 1999; Hogg et al. 2006; Edmands 2007; Hedrick and Fredrickson 2009; Bijlsma et al. 2010; Holmes et al. 2008; Bell et al. 2019). In the case of the Florida panther, an estimated genetic replacement of ~41% has been reported (Johnson et al. 2010). In another case of the Isle Royale wolf, the immigration of one single male to Isle Royale caused a genetic replacement of 56% to the local inbred population within two generations (Adams et al. 2011; Hedrick et al. 2019). Furthermore, Hwang et al. (2012) reported negative fitness effects in cases of GR between genetically highly divergent species due to outbreeding depression.

Several different theoretical studies have been conducted to examine the expected efficacy of GR (Tallmon et al. 2004; Frankham et al. 2011; Hedrick et al. 2016; Harris et al. 2019). The dynamics of GR are complex, depending on, among other factors, the amount of gene flow, the demographic history (e.g. effective population size), and the dominance coefficients of mutations. Harris et al. (2019) demonstrated that higher levels of assisted admixture could lead to a more rapid recovery in the relative fitness of the recipient population; however, this occurs at the cost of replacing an increasing proportion of the recipient's ancestral genomes with those of the donor population. Such effects would be maximized when deleterious mutations are recessive (Kim et al. 2018; Harris et al. 2019). The demographic history of both the recipient and donor populations also shape the dynamics of GR. For instance, small effective population size (N_e) limits the efficacy of natural selection; thus, in most cases, admixture from a population with large N_e helps restore fitness (Harris et al. 2019; Fitzpatrick et al. 2020). However, several studies have revealed that demography and dominance of deleterious mutations have key interaction effects on the GR process (Xue et al. 2015; Robinson et al. 2016; Harris et al. 2019; Kyriazis et al. 2021). For example, Kyriazis et al. (2021) showed that GR from populations

with historically low N_e can be more robust to the effects of severe bottlenecks in the recipient population than those with historically large N_e. The underlying assumption is that historically large populations could carry more strongly deleterious recessive mutations, which are most sensitive to extreme bottlenecks, in heterozygote state while smaller populations are more efficient at purging these mutations.

Previous studies suggest that the genetic replacement caused by GR can be controlled if the amount of admixture is limited (Whiteley et al. 2015; Bell et al. 2019; Harris et al. 2019). However, whether local adaptation plays a role in GR remains an open question. Specifically, whether GR would lead to the loss of unique local adaptations, or whether local adaptations could affect the process of fitness restoration by GR, remain largely unexplored.

Here, we explore how the addition of linked locally adaptive variation affects the GR process. Specifically, we explore the dynamics under GR on 1) Mendelian traits, and 2) polygenic traits under stabilizing selection with a shift in the optimum. Our results illustrate how the genetic architecture of adaptive traits evolve under GR, and how the dynamics of GR depend on the joint effects of demographic history and genetic factors such as dominance.

Methods

We simulated two demographic models from Harris et al. (2019), as illustrated in Fig. 1A and B. The simulations were conducted using SLiM v3.2 (Haller and Messer 2019). Model 1 (Fig. 1A) represents a population that undergoes a long-term bottleneck of 0.1 times the ancestral population size ($N_e = 10^4$), which lasts for 16,000 generations. This demographic history represents a population that is small for a long period of time and has a similar history to Neanderthals as inferred by Prufer et al. (2014). Neanderthals represent a good example of a long-term inbred population where genomic analyses have discovered a substantial accumulation of deleterious alleles (Castellano et al. 2014; Prufer et al. 2014). Model 2 (Fig. 1B) represents instead a population with an extreme, short-lived bottleneck with $N_e = 10$ that lasts for 20 generations, which might be more representative of many currently endangered species (Miller et al. 2020). To further explore the dynamics of GR under different demographic parameters in Model 2, we varied the divergence time between the donor and recipient populations (Fig. 1C) and the extent of population size recovery after GR in the recipient population (Fig. 1D). Prior to the time of divergence, we conducted a burn-in phase of 44,000 generations. We simulated two trait architectures: a Mendelian trait, with only one adaptive site contributing to the trait, and a polygenic trait with a large mutational target.

We simulated the Mendelian trait under two selection models: 1) a hard sweep, in which a rare additive beneficial mutation occurs after the split of the population, and 2) a soft sweep from a standing variant, in which an allele segregating until the split is picked at random, and its selection coefficient is then changed so that the allele becomes

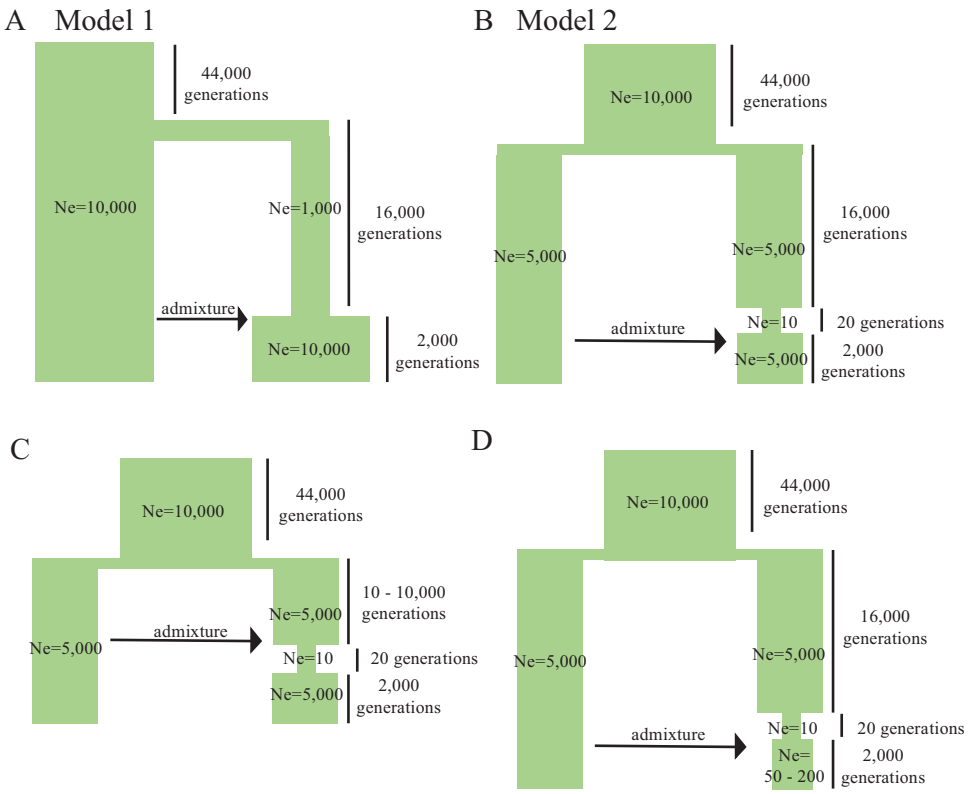

Fig. 1. Demographic models used for simulations. A) shows demographic Model 1 with a long-term bottleneck. B) shows demographic Model 2 with a short-term extreme bottleneck. Demographic Model 2 is further explored by varying the divergence time between the donor and recipient populations C) and the recipient population size after GR D). Time runs from top to bottom. Admixture happens at the generation right after the population size increases and lasts for only one generation. Population size changes are assumed to be discrete as depicted in the figure. Samples are taken from the recipient population on the right after the admixture up to 2,000 generations.

beneficial. Selection acts on the trait only after the split of two populations. For both models, we examined multiple selection coefficients for the adaptive alleles, including $s = 10^{-4}$, 10^{-3}, and 10^{-2}.

We simulated the polygenic trait under a model of stabilizing selection with Gaussian fitness. To model the effects of local adaptation in the recipient population, we allowed the phenotypic optimum in this deme to increase by some amount, immediately following the divergence from the ancestral population. With V_s as the variance (width) of the fitness function (not to be confused with the variance in fitness among individuals), we simulated scenarios where the inbred population's phenotypic optimum shifts by δ = 1, 2, 5 immediately after the split, while the phenotypic optimum remains at 0 for the outbred population. The fitness of the polygenic trait is thus calculated as

$$f(p) = \frac{1}{\sqrt{2\pi V_s}} e^{-\frac{(p-\delta)^2}{2V_s}},$$

where the phenotypic value (p) is calculated as the sum of effects (a) of casual alleles $p = \sum_{i \in \mathrm{SNPs}} a_i$. We considered different selection strengths by setting the variance of the fitness function to be V_s = 3,000 and 10,000. We assume genetic effects among loci are additive. Under this model, at equilibrium (phenotypic mean equals to the optimum), alleles are under under-dominant selection with $s = a^2/V_s$, where a is the effect of the allele, on the same scale on which the fitness function is defined (Simons et al. 2018). In the transient phase after a large shift in the optimum, selection is approximately additive with $s = a\delta/V_s$ (Hayward and Sella 2022). We assume selection coefficients of causal single nucleotide polymorphisms (SNPs) to be roughly $s \sim 10^{-4} - 10^{-3}$, in line with current estimates that SNPs associated to complex traits in humans have been under weak selection (Simons et al. 2018). We draw the effects of causal alleles (a) from a standard normal distribution (i.e. mean = 0 and variance = 1). See Supplementary Table S1 for more details.

In addition to the adaptive mutations described above, we also allowed for accumulation of deleterious mutations assumed to be 1) additive (h = 0.5), 2) partially recessive (h = 0.1), and 3) recessive (h = 0), where h is the dominance coefficient. To specify a set of simulation parameters realistic for mammals, we chose parameters inferred in humans for recombination rates and distribution of fitness effects (DFE). We simulated whole human exome sequence (~71.5 Mbp) using the UCSC exon recombination map from the human reference genome (build: hg19) and a DFE on non-synonymous mutations—a gamma distribution with a mean of –0.043 and shape parameter α = 0.23, estimated by (Eyre-Walker et al. 2006). We assumed a non-synonymous mutation rate of 7×10^{-9} per bp/generation, based on an estimate of 1.0×10^{-8} mutations per site per generation (1000 Genomes Project 2010; Scally and Durbin 2012) and approximately two-third of mutations in coding regions leading to changes in amino acid sequence (Harris and Nielsen 2016), and log additive interactions among selected loci. A summary of the simulations is provided in Supplementary Table S1.

For all simulations, we recorded mean fitness over all individuals in the recipient population relative to that of the outbred population, the ancestry proportion in the inbred recovering population, the varying allele frequency of the adaptive mutation in the Mendelian model, and the fluctuation of mean phenotype in the stabilizing selection model.

Results

Fitness changes and genomic replacement after GR

We explored the dynamics of GR on the fitness and ancestry fraction of the recipient population under different demographic models (Fig. 1A and B) and demographic parameters of Model 2(Fig. 1C and D), assuming different dominance coefficients of deleterious variations, different admixture proportion during GR and two types of adaptive traits (Mendelian and polygenic). Fitness is measured by taking the average of the individual fitness of offspring in the recipient population and normalized by the same quantity for the donor population. The fitness calculated in generation T is the fitness of parents (rather than offspring) in generation T.

We first investigated the effects of GR on fitness and ancestral genome reduction in the recipient population depending on the severity and length of the bottleneck (i.e. Model 1 vs. Model 2, Fig. 1A vs. B). Consistent with our previous results (Harris et al. 2019), we found that, under different demographic models and dominance of deleterious variation, GR has drastically varying rates of success (in terms of achieving a rapid increase in relative fitness). When deleterious mutations are additive, GR only acts successfully in Model 1, where a certain amount of fitness reduction is shown before GR (Fig. 2A, Supplementary Fig. S2A and D). In contrast, when deleterious mutations are partially recessive, GR is successful in both models albeit much faster under Model 2 (Fig. 2B, Supplementary Fig. S2B and E). We observed extensive heterotic effects under a fully recessive load: provided sufficient admixture (1%), the recipient population fitness increases relative to that of the donor population in Model 2 in 10 generations, whereas in Model 1 the fitness is not restored to the same level even in the long run (>1,000 generations post-GR) (Fig. 2C, Supplementary Fig. S2C and F). Generally, we found that the lower the recipient fitness before GR, the higher the amount of genomic replacement by the donor population in the long run. Furthermore, the more successful GR is at restoring fitness, the higher the amount of genomic replacement in the long run (Fig. 2D–F, Supplementary Fig. S3). Our results align with previous empirical studies on *Drosophila melanogaster*, demonstrating that the post-GR fitness increase can persist for over 10 generations, with a larger fitness increase observed when the recipient population has lower initial fitness (Bijlsma et al. 2010).

A short-term bottleneck (Model 2) does not increase or decrease the average number of mutations an individual carries. However, it allows recessive deleterious mutations of strong deleterious effects that were segregating in the population to increase in frequency and potentially go to fixation (while others are lost). Models with recessive mutations allow for much more standing variation of deleterious mutations that potentially can increase in frequency during the bottleneck compared with models with additive mutations (e.g. Fig. 2A vs. 2C). GR is, therefore, particularly effective in the presence of short-term bottleneck and recessive deleterious mutations, because the recipient population may have fixed strongly deleterious recessive mutations that can be purged immediately after GR (Fig. 2C). In the case of a constant low population size (Model 1),

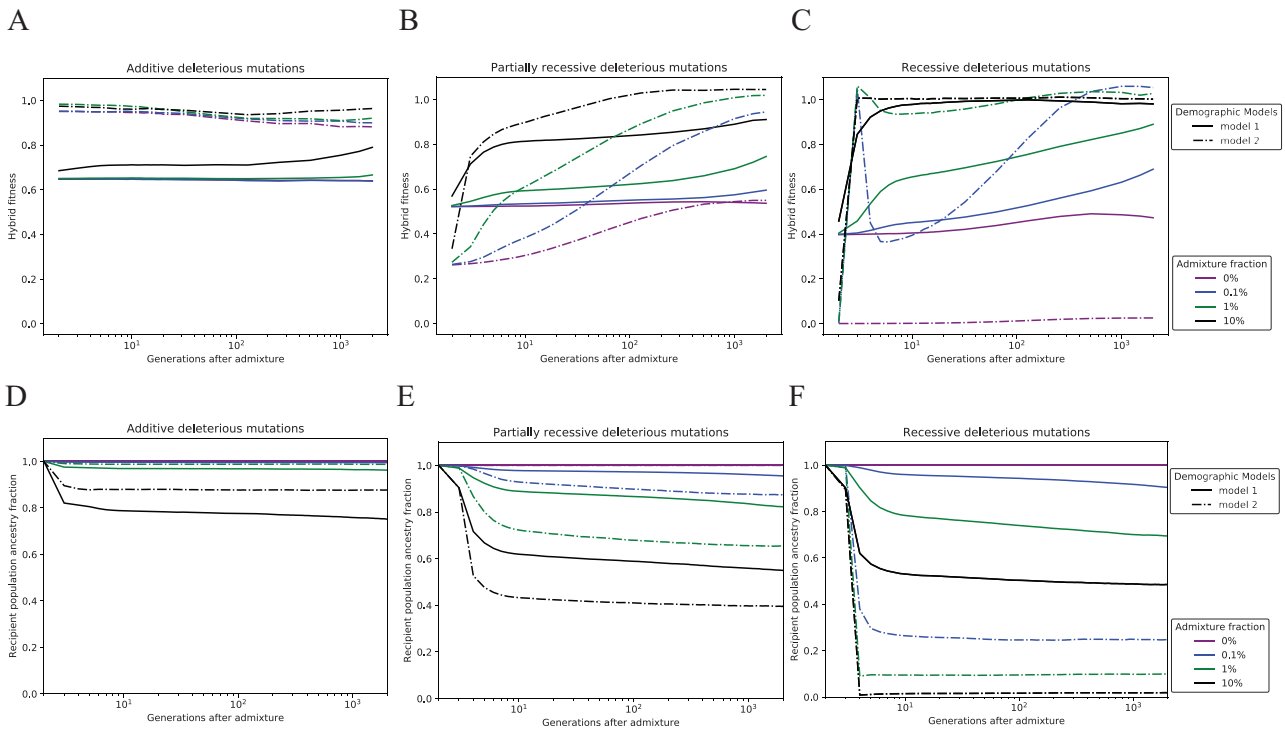

Fig. 2. A–C) Relative fitness (of the recipient population to donor population) change of the recipient population after admixture and D–F) Recipient population ancestral genome fraction changes after GR with a Mendelian adaptive trait, under hard sweep selection model and demographic Model 1 (solid lines) and demographic Model 2 (dashed lines). Averaged values of 10 simulation repeats are shown in trajectories. The adaptive mutation is additive (dominance coefficient $h = 0.5$). Deleterious mutations are assumed additive ($h = 0.5$) in A and D, partially recessive ($h = 0.1$) in B and E, and recessive ($h = 0$) in C and F.

deleterious mutations (both in the recessive and additive model) will accumulate and can slowly go to fixation if they have weak effects, but one is unlikely to observe the same kind of strong effect of strongly deleterious recessive mutations going to fixation as that would be seen in models with recessive mutations and a severe bottleneck (Fig. 2B and C).

We further illustrated the joint dynamics of fitness recovery and genetic replacement under a severe bottleneck (Model 2) with recessive deleterious mutations in Fig. 3. We found that in the first generation after GR, native ancestry is either 0% or 100% in the parents, where 100% native ancestry is associated with much lower fitness (Fig. 3A). After one generation of admixture between donor individuals and the recipient population, a large proportion of offspring have hybrid genomes (with one inbred and one outbred chromosome), despite a low admixture proportion (1%). The hybrid individuals enjoy much higher fitness than inbred individuals, as well as the non-crossed outbred individuals, because it is extremely rare for the hybrid individuals to be homozygous for recessive deleterious variation (as it would require a recessive deleterious variant to segregate in both inbred and outbred populations at the time of the assisted admixture, e.g. GR). In the following generations, as ancestry proportions range between ~30% and 90%, there is a clear trend of lower native ancestry incurring increased fitness in the recipient population (Fig. 3C and D).

The extent of the heterosis effect under Model 2 is impacted not only by the dominance of deleterious mutations, but also by the length of divergence between donor and recipient populations before GR. As shown in Fig. 4D–F, under the same scenario assuming deleterious mutations being partially recessive or recessive, fitness in the recipient population recovers more rapidly immediately after GR (<10 generations) with a longer divergence time between the two populations (Fig. 4E and F, Supplementary Fig. S7). On the contrary, we noticed a reduced degree of local genetic ancestry replacement with greater divergence, possibly because of the increased genetic heterogeneity between the two populations (Fig. 4F, Supplementary Fig. S7).

We also examined the impact of population size recovery after GR on the recipient population fitness restoration and ancestry maintenance. Compared with scenarios where the recipient population size fully recovers (to its pre-bottleneck value, $N_e = 5{,}000$, Fig. 2), we observed recurrent inbreeding depression in scenarios assuming smaller constant N_e values after GR (Fig. 4A–C, Supplementary Fig. S6). Generally, we found that populations with smaller increases in N_e after GR have more significant recurrent fitness reduction in the long run. Furthermore, the more successful GR is at restoring fitness, the greater the local ancestry loss observed in the recipient population (Fig. 4A–C, Supplementary Fig. S6). The timing and extent of recurrent inbreeding depression are dependent on the dominance effect of deleterious mutations. When deleterious mutations are additive, GR has no effect on the recipient population, and fitness decreases slowly, with only about a 10% reduction observed in the long term (>100 generations after GR, Fig. 4A, Supplementary Fig. S6A and D). In contrast, when deleterious mutations are partially recessive, GR succeeds at short-term fitness restoration (10 generations post-admixture), followed by a long-term fitness decline (Fig. 4B, Supplementary Fig. S6B and E). This pattern is even more extreme in cases

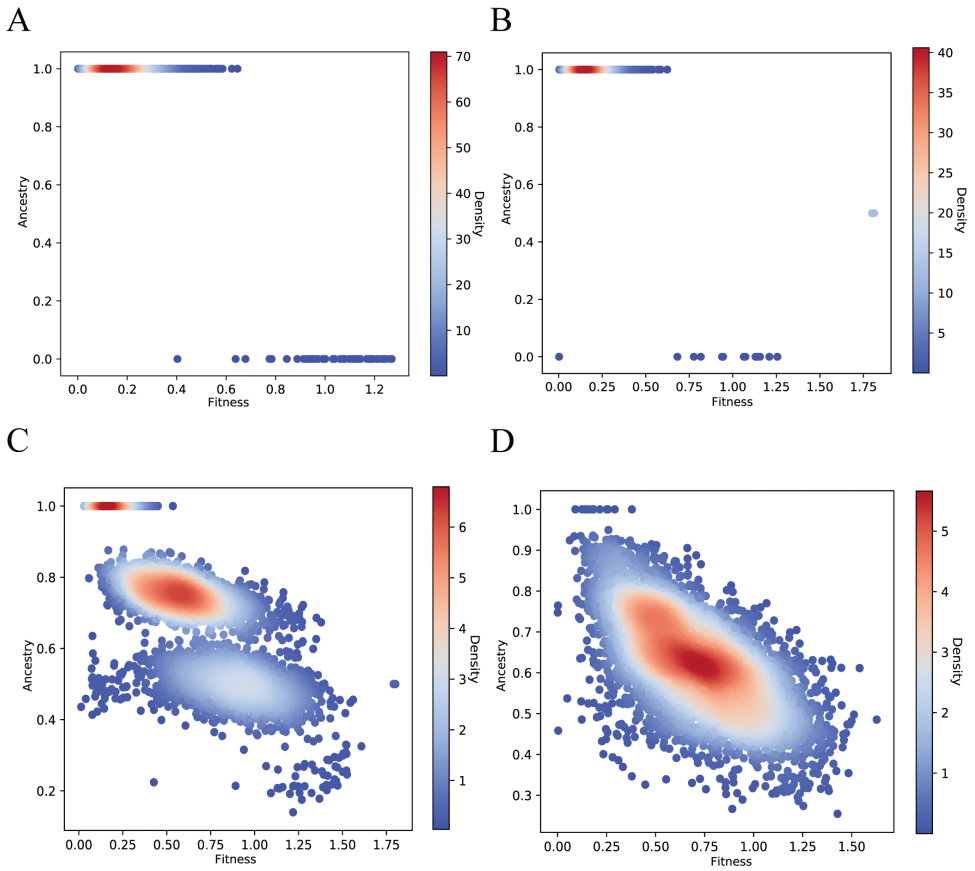

Fig. 3. Relation between individual fitness and its ancestral genome proportion under demographic Model 2, with recessive deleterious mutations and admixture fraction of 1%. Each dot represents an individual, depicting the relation between ancestry proportion and relative fitness (to the mean fitness of the outbred population) of each individual in the inbred recipient population. A) shows the population before mating with outbred individuals. B) indicates the first generation after admixture (e.g. F1), while C) represents the second generation (e.g. F2), and D) shows the third generation (e.g. F3).

with a recessive mutation load: given a substantial amount of admixture (10%), fitness recovers only in the first generation post-admixture, followed by a steep fitness reduction in the next generation, and gradual reduction (more rapid than that observed Fig. 4B) afterward. In the scenario where the population size increases fivefold after GR (N_e = 50), hybrid fitness returns to its pre-GR value in approximately 20 generations (Fig. 4C, Supplementary Fig. S6C and F).

Lastly, we directly compared the recipient population fitness (hybrid fitness) trajectories under Mendelian and polygenic trait models (Supplementary Figs. S1–S7 vs. S8–S11). We found that under the simulation models we considered, varying parameters controlling the local adaptation (e.g. hard or soft sweep model and selection coefficient for the Mendelian trait and optimum and variance terms for the polygenic trait) do not have any appreciable effect on fitness as an outcome of GR. In Supplementary Fig. S1 we compare simulations of a Mendelian trait under strong selection (Supplementary Fig. S1A and B) vs. a polygenic trait under strong stabilizing selection (Supplementary Fig. S1C and D). The results are comparable both under Model 1 (Supplementary Fig. S1A and C) and Model 2 (Supplementary Fig. S1B and D) and under various levels of dominance (Supplementary Fig. S1).

Selection on Mendelian traits

We simulated a Mendelian trait that is fixed for the derived (locally adaptive) allele in the recipient population, and fixed for the ancestral allele in the donor population. We varied the selection coefficient of the trait, the dominance coefficient of the linked deleterious variation, the admixture proportion during GR, the demographic model including a long-term small effective population size (Model 1) and a short-term severe bottleneck model (Model 2), and demographic parameters including the divergence time between populations and effective population size after GR (see Fig. 1).

First, we looked at the dynamics of local adaptations under different demographic settings (Figs. 5 and 6, Supplementary Figs. S12 and S13). We found that, in the short term (~10 generations post-GR) the adaptive allele decreases in frequency following the loss of ancestral variation (Fig. 5 vs. 2; Fig 6 vs. 3), which is the consequence of selection being dominated by the global influence of deleterious mutations in native ancestry after the assisted admixture of GR (Figs. 2 and 3). In most scenarios we explored, the adaptive allele starts increasing in frequency in 10 generations when enough recombination occurs to break up the linkage between the adaptive allele and the deleterious alleles. However, even for very strong selection (s = 0.01), it takes hundreds of generations for the adaptive allele to fully restore (to fixation) in the recipient population, which is beyond the limit of empirical experiment records (Figs. 5 and 6, Supplementary Figs. S12 and S13). In some extreme cases, with sufficiently high levels of admixture (10%), GR under Model 2 actually causes the adaptive allele to be lost with high probability after a total genetic replacement in

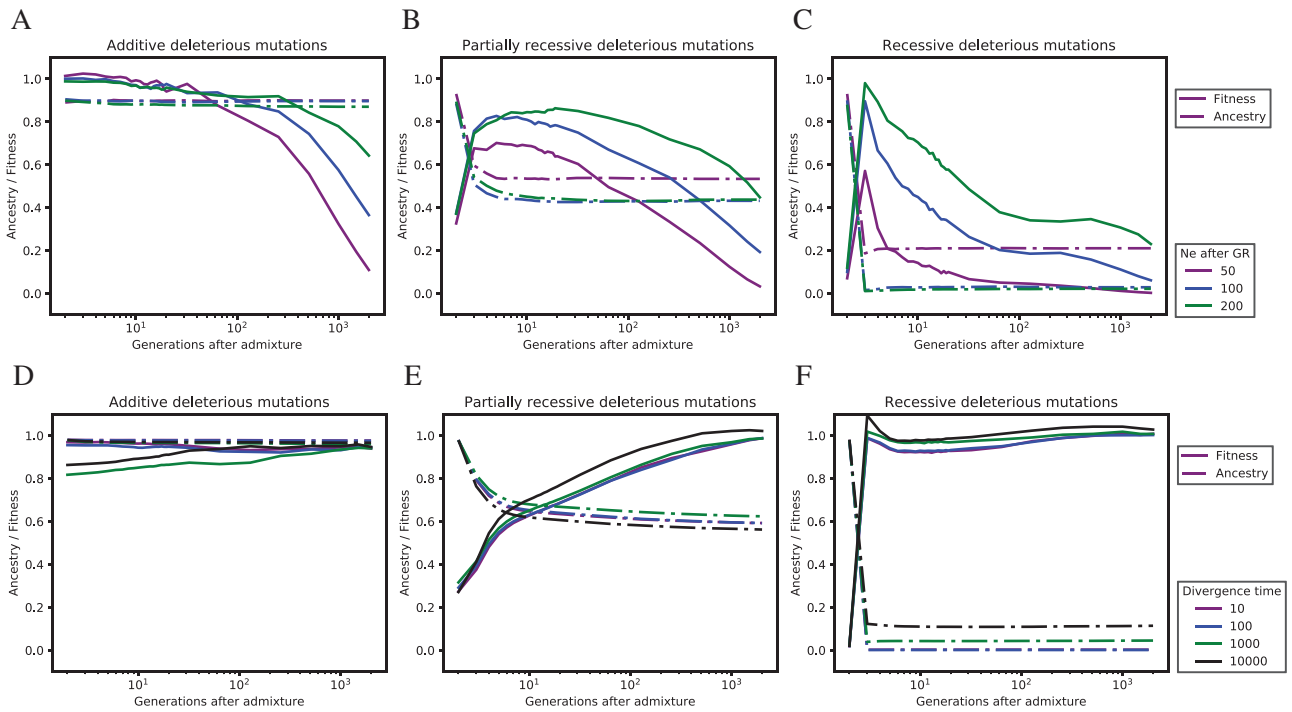

Fig. 4. Relative fitness (of the recipient population to donor population) and ancestral proportion change of the inbred population after GR under demographic Model 2 assuming A–C) different extents of effective population size recovery and D–F) different lengths of divergence between donor and recipient populations, under a soft sweep selection model with 10% A–C) and 2% D–F) admixture between populations. Averaged values of 10 simulation repeats are shown in trajectories. Deleterious mutations are assumed additive ($h = 0.5$) in A and D, partially recessive ($h = 0.1$) in B and E, and recessive ($h = 0$) in C and F.

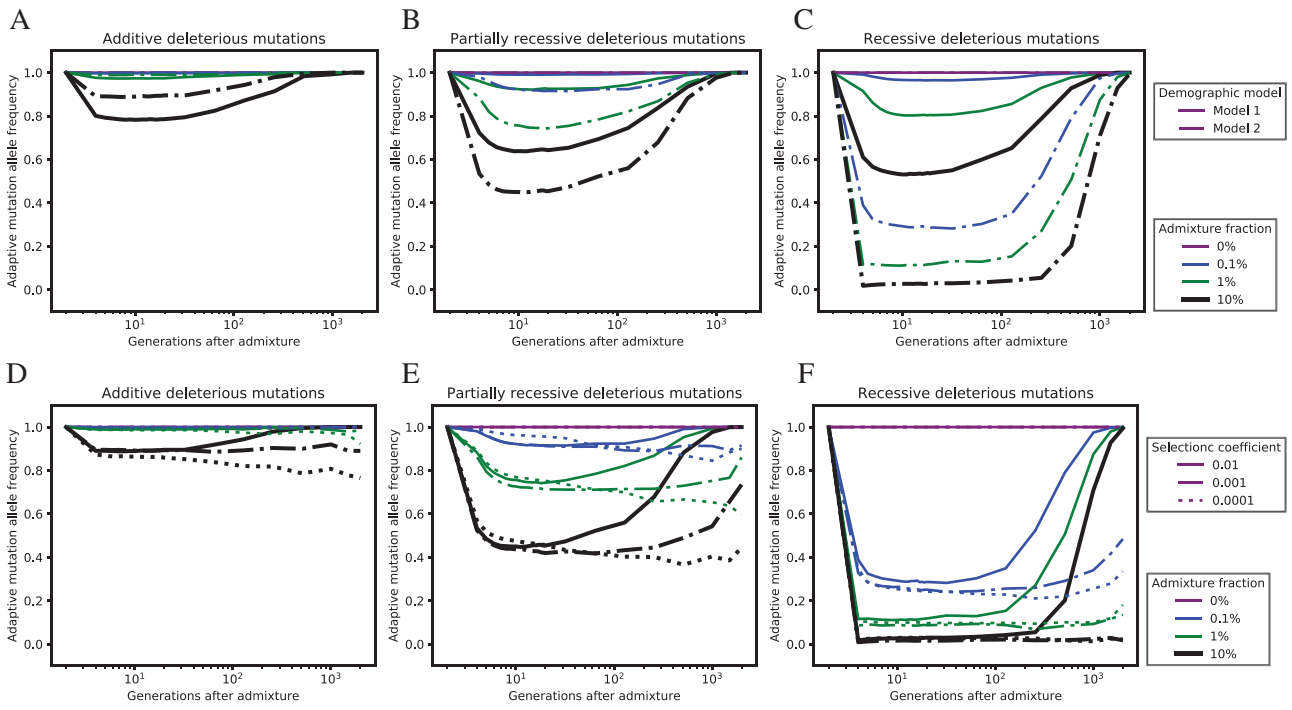

Fig. 5. Allele frequency changes after admixture for a Mendelian trait under hard sweep positive selection model. A–C) show results of relatively strong selection ($s = 0.01$) under different demographic models and D–F) for different selection strengths under demographic Model 2. Averaged values of 10 simulation repeats are shown in trajectories. The adaptive mutation is additive (dominance coefficient $h = 0.5$). Deleterious mutations are assumed additive ($h = 0.5$) in A and D, partially recessive ($h = 0.1$) in B and E, and recessive ($h = 0$) in C and F.

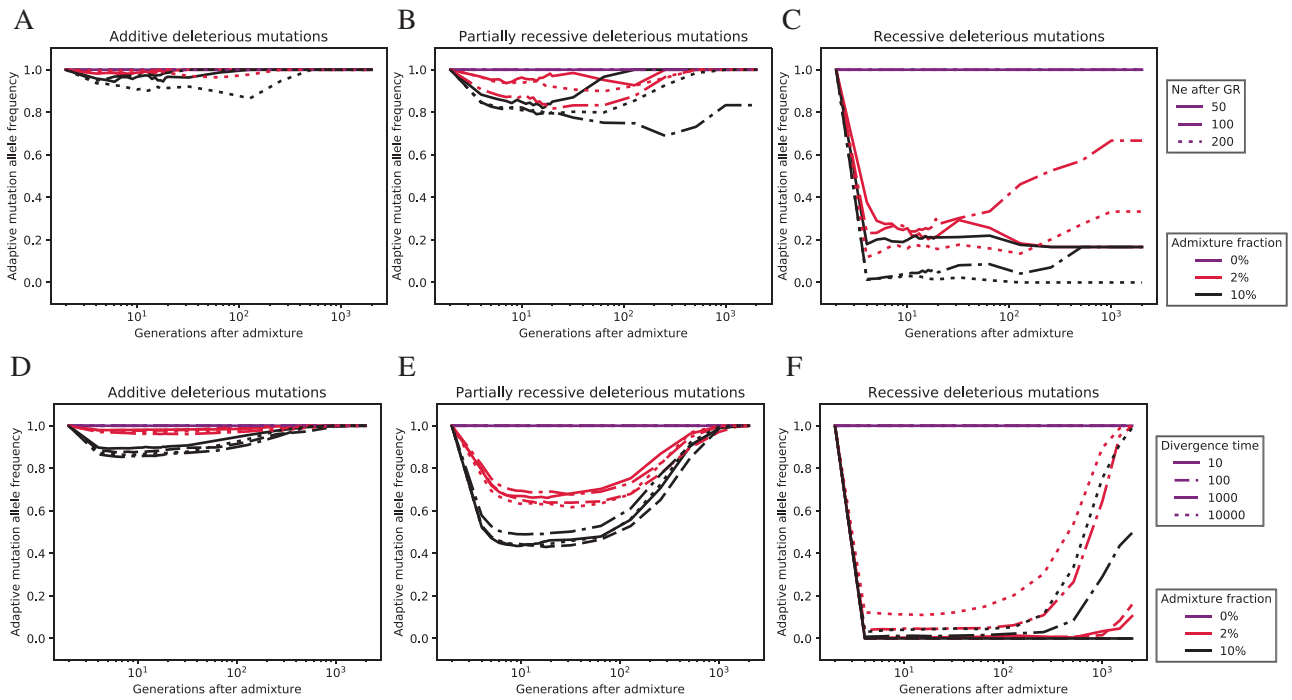

Fig. 6. Allele frequency changes after admixture for a Mendelian trait under soft sweep positive selection assuming demographic Model 2. A–C) show results of varying recipient population size after GR and D–F) varying divergence time between populations before GR. Averaged values of 10 simulation repeats are shown in trajectories. The adaptive mutation is additive (dominance coefficient $h = 0.5$) and relatively strongly selected (selection coefficient $s = 0.01$). Deleterious mutations are assumed additive ($h = 0.5$) in A and D, partially recessive ($h = 0.1$) in B and E, and recessive ($h = 0$) in C and F.

scenarios when the selection coefficient is sufficiently small (≤0.001, Fig. 5F), the population size of the recipient population after GR stays limited (N_e = 50, 100, or 200, Fig. 6C), or the divergence time between the donor and recipient population is short (<1,000 generations, Fig. 6F).

We also examined the joint effects of dominance coefficients of linked deleterious variation and demographic history on the efficacy of GR. In all simulations under different demographic settings, we saw a greater degree of genetic replacement (Figs. 2 and 3), leading to a greater reduction in the frequency of the adaptive allele, as deleterious mutations become more recessive (Figs. 5 and 6, Supplementary Figs. S12 and S13). For example, there was a smaller short-term reduction in allele frequency of the adaptive allele under Model 2 relative to Model 1 when deleterious variants are additive (Fig. 5A, Supplementary Figs. S12 and S13A,D) but a larger reduction for partially recessive or recessive deleterious variants (Fig. 5B,C,E,F, Supplementary Figs. S12 and S13B,C,E,F), following the same pattern of the ancestral variation proportion decline in those scenarios (Fig. 2D–F, Supplementary Fig. S3). However, the locally adaptive locus itself had only a minor effect on the recovery of relative fitness and reduction of ancestral DNA proportion of the recipient population (Supplementary Figs. S1, S2, S4). These results emphasize the importance of weakly deleterious mutations in shaping the genetic architecture rather than strongly adaptive mutations, which is consistent with previous simulation studies and observations in modern human genomes (Lohmueller et al. 2011; Kim et al. 2018).

We considered that sweeps from standing variation may have different patterns of linked deleterious variation around the adaptive allele; however, when simulating under alternative selection models we found no difference between the hard vs. soft sweep models (see Fig. 5, Supplementary Fig. S13 vs. S14; Supplementary Figs. S2, S3 vs. S4, S5).

Polygenic adaptation

We also simulated a polygenic trait under a model of stabilizing selection with a shift in the optimum (Figs. 7 and 8). Here we varied the strength of stabilizing selection on the trait (controlled by $\sqrt{V_s}$, the "width" of the fitness function), the size of the shift in the local optimum after the divergence of donor and recipient populations, δ = 0, 1, 2, 5, measures in units of $\sqrt{V_s}$, the dominance coefficient of deleterious mutations, the admixture fraction during GR, as well as the demographic model.

We examined two features of polygenic trait evolution: first, we evaluated the effect of GR on the perturbation of the adaptive phenotype from its optimum (Fig. 7, Supplementary Fig. S16); we measured this by looking at the average distance of the population mean phenotype from the optimum. We also considered the extent of replacement of ancestral variation associated with the trait (Fig. 8, Supplementary Fig. S17); we measured this replacement by examining the relative proportion of genetic variance of the trait due to ancestral variation vs. donor variation introduced by GR.

We found that under Model 1, polygenic adaptations are not significantly affected by GR, as the trait`s evolution appears to follow the same trajectory regardless of admixture proportions or dominance coefficients of the deleterious load (Fig. 7A–C, Supplementary Fig. S16A–C). However, under Model 2, we found that following rapid phenotypic drift from the optimum due to a severe bottleneck, polygenic adaptations subsequently follow dramatically different trajectories depending on several factors (Fig. 7D–F, Supplementary Figs. S15, S16D–F): for example, GR allows

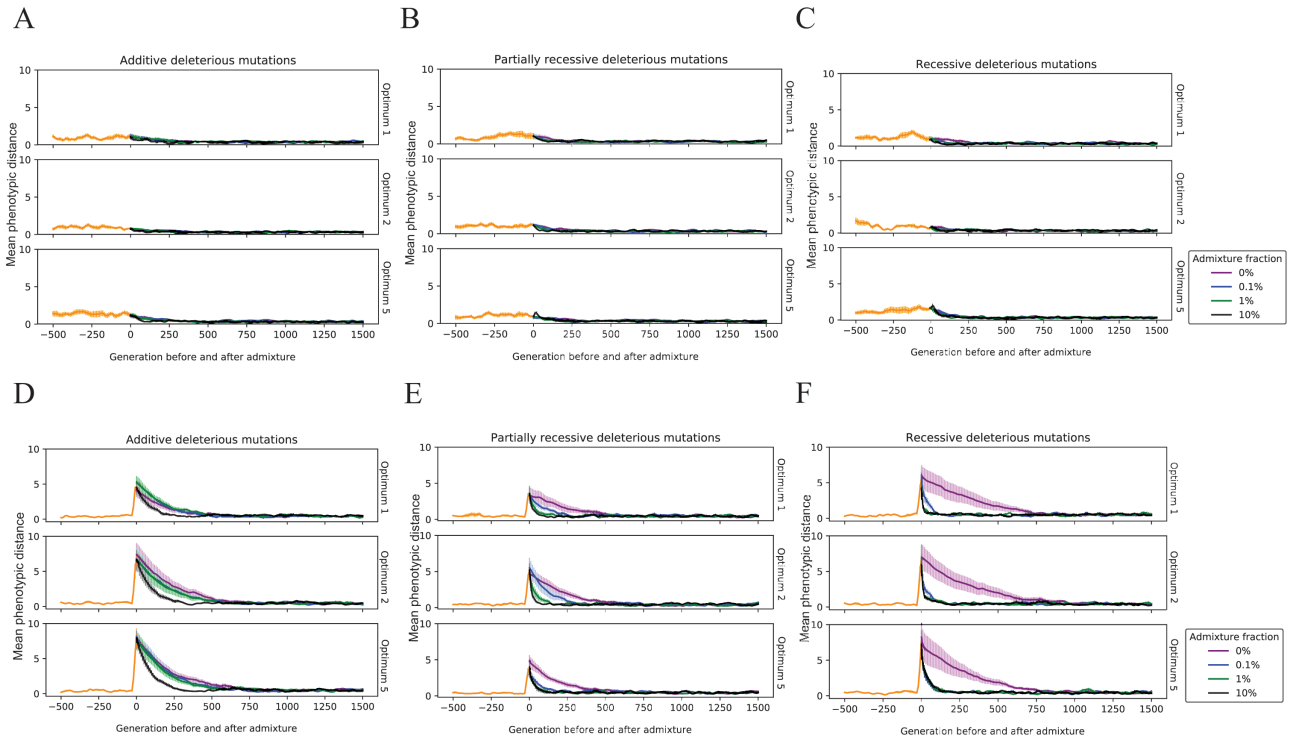

Fig. 7. Mean phenotype distance from optimum over time. A–C) Simulations under Model 1, D–F) simulations under Model 2. Shaded bars show the 95% confidence intervals of the mean phenotypic distance in 10 simulation repeats.

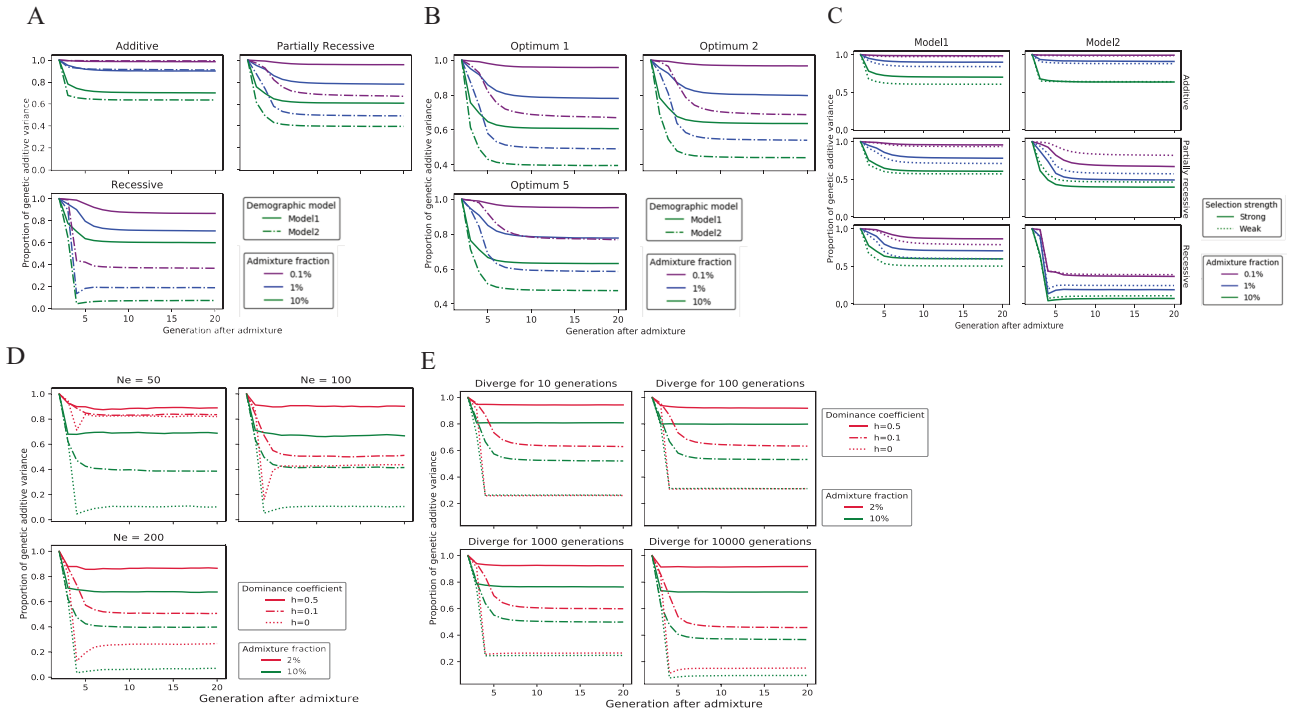

Fig. 8. Proportion of the polygenic trait (genetic additive variance of mutations that compose the trait) that originate from the recipient population after GR. A) Effects of different dominance coefficients for deleterious mutations on the polygenic trait, assuming strong selection and a phenotypic optimum of 1 for the recipient population. B) Effects of different phenotypic optimums for the recipient population on the polygenic trait, assuming strong selection and partially recessive deleterious mutations. C) Effects of selection strength on the polygenic trait assuming a phenotypic optimum of 1. D) Effects of population size recovery after GR on the polygenic trait, assuming strong selection, phenotypic optimum of 1 under demographic Model 2. E) Effects of length of divergence between populations on the polygenic trait, assuming strong selection, phenotypic optimum of 1 under demographic Model 2. Each line represents the proportion of genetic additive variance contributed by variants, which compose the trait, from the ancestral genome of the inbred population. Here, genetic additive variance is calculated as $\boldsymbol{G} = \sum_{l \in \mathrm{SNPs}} 2a_l^2 p_l(1 - p_l)$, where a_l represents the effect of SNP l, and p_l its frequency.

the polygenic adaptation to recover to its optimal value much more quickly than without GR assuming a full population size recovery (Fig. 7D–F, Supplementary Fig. S16D–F); and this effect is most pronounced under scenarios where there is fully recessive load (Fig. 7F, Supplementary Fig. S16F), although it is still significant under a partially recessive load (Fig. 7E, Supplementary Fig. S16E). When the recipient population size stays limited after GR, the phenotypic drift from the optimum continues and polygenic adaptations are primarily influenced by the population size rather than GR (Supplementary Fig. S15A–C). We found no significant impact of divergence time between donor and recipient populations on dynamics of polygenic adaptations after GR under Model 2 (Supplementary Fig. S15D–F).

We also explored how the genetic basis of the polygenic adaptation in the recipient population is replaced by donor variation (Fig. 8, Supplementary Fig. S17). We quantify this using the proportion of the genetic variance attributable to standing variation in the recipient population just before admixture; genetic variance post-admixture is the sum of this quantity, plus genetic variance attributable to standing variation in the donor population just before admixture, plus that of de novo mutations occurring in the recipient population post-admixture (although this has negligible contributions over short timescales). Generally, we find that the genetic basis is quickly replaced due to GR, with >90% of the genetic variance being replaced with donor variation when GR is most successful; for example, under Model 2, especially when the deleterious load is recessive and the admixture fraction is high (Fig. 8A, Supplementary Fig. S17A). Broadly, patterns of genetic variance replacement are consistent with patterns of ancestry replacement (Fig. 8, Supplementary Fig. S17 vs. S9–S11), with stronger replacement in situations where GR is more successful at recovering fitness. However, details of the local adaptation do affect the dynamics of how the genetic variance evolves; for example, when the optimal phenotypes differ substantially between the recipient and the donor population, the fraction of the genetic variance replaced by the donor population is lower (Fig. 8B, Supplementary Fig. S17B), because in this case donor individuals are more poorly adapted to the environment of the recipient population, and thus GR is countervailed by this force.

Discussion

We present a population genetic simulation study that elucidates the dynamics of local adaptation and GR, considering various models of the selection strength and architecture of the adaptive trait, dominance of the mutational load, demography, and admixture fractions. The results of our simulations show that generally, GR helps restore population fitness following assisted migration, with fitness increases observed within ten generations, in most cases. But as the efficacy of GR increases, so does the amount of genomic replacement in the recipient population.

Despite the success at overcoming inbreeding depression in the short term, insufficient population size recovery will lead to recurrent inbreeding depression and to a failure of GR in the long term. When most deleterious mutations are recessive in the genome, performing GR in an inbred population that has gone through a short and severe bottleneck, will likely cause a complete genetic replacement and a subsequent recurrence of inbreeding depression, unless followed by rapid population size growth. We also note that repeated GR, which is not modeled here, has the potential to negatively impact the fitness of the recipient population by repeatedly introducing recessive deleterious alleles, thereby negating the effects of purging.

Our results highlight the importance of reassessing feasibility before implementing GR in populations confronting ecological threats, such as habitat loss, which might hinder population expansion post-GR.

When a locally adaptive trait consists of a single locus (e.g. a Mendelian trait), GR decreases the allele frequency in the short term. The dominance of the linked deleterious variants and the demographic history of the population jointly determines the degree of its short-term loss while the strength of positive selection determines the rate of trait recovery. In our simulations, although the adaptive allele frequency might continue to decrease in the scope of empirical experiments (10 generations after GR), the chance of losing the adaptive trait completely is very small: we only observed this in very extreme scenarios where the deleterious mutations are all recessive and the adaptive advantage of the trait/population size after GR/divergence between populations is sufficiently small. Our results are consistent with observations in empirical experiments on wild guppy populations that gene flow can increase the fitness of small populations without erasing adaptive variation (Fitzpatrick et al. 2020).

There are substantial differences in the evolutionary dynamics of Mendelian and polygenic traits under GR. Our simulations of polygenic traits show that the consequences of GR on the trait were driven by both the loss of genetic variation as a whole and the distance between the phenotype and its optimum before GR. In general, it takes a long time (about 100 generations, beyond the scope of empirical experiments) for a polygenic trait to return to its optimum in most cases. Failure of the recipient population to recover to a healthy population size can result in continued deviation of the trait from its optimum. Because polygenic traits have a large mutational target, causal genetic variation that was previously exclusive to the donor population is introduced to the inbred population via GR; this variation quickly replaces native causal genetic variation, which is linked to many deleterious alleles. Thus, the apparently higher efficiency with which the polygenic adaptation is restored comes at the cost of long-term replacement by genetic variation from the donor population. We also showed that the distance of the phenotypic optimum between the donor and the recipient population has an appreciable influence on how much genomic replacement is incurred by GR.

Our results not only illustrate the short-term effects of GR, but also predict the long-term genetic future of the recipient population (over hundreds of generations after GR), which is usually beyond the scope of empirical experiments. Additionally, we dissected the impact of various critical factors, including demographic history, genetic architecture of adaptive traits, and dominance effects of mutation load, individually and in combination, enabling us to untangle the effects of complex genetic features observed in empirical data.

One caveat of our results is that although we have included scenarios assuming different extents of divergence between the donor and recipient populations, our simulations do not assume epistasis and, therefore, do not allow for the evolution of Dobzhansky-Muller incompatibilities (DMIs). However, in the presence of DMIs, outbreeding depression may lead to

limited genetic replacement or even reduce the absolute fitness after GR.

Our simulations highlight the advantages and risks of GR under various demographic settings and genetic architecture. Although our results suggest that locally adaptive traits, especially those that are Mendelian or moderately polygenic, will be strongly affected by GR in the short term, the causal variant is generally retained and returns to fixation in the long run. While locally adaptive polygenic traits are less susceptible to shifts due to GR, their underlying genetic architecture is highly susceptible to long-term replacement by donor ancestry.

Supplementary material

Supplementary material is available at *Journal of Heredity* Journal online.

Acknowledgments

We would like to thank Bob Wayne for stimulating discussion that lead to the initiation of this research project and for his enduring service and enthusiasm for the use of genetics in conversation biology that helped inspire this research. We thank Priya Moorjani for her comments on the manuscript.

Funding

This work was supported by the National Science Foundation (DEB 1655336) and the National Institutes of Health (R01GM138634). Yulin Zhang was supported by the National Institutes of Health Maximizing Investigators' Research Award (R35GM142978) and Hellman Family Faculty Fund to Ph.D. supervisor Priya Moorjani.

Conflict of interest statement. None declared.

Data availability

Scripts are available on GitHub at https://github.com/YulinZhang9806/GR_adaptation_scripts.

References

1000 Genomes Project Consortium. A map of human genome variation from population scale sequencing. Nature. 2010:467:1061.

Adams JR, Vucetich LM, Hedrick PW, Peterson RO, Vucetich JA. Genomic sweep and potential genetic rescue during limiting environmental conditions in an isolated wolf population. Proc R Soc B. 2011:278:3336–3344.

Bell DA, Robinson Z, Funk WC, Fitzpatrick SW, Allendorf FW, Tallmon DA, Whiteley AR. The exciting potential and remaining uncertainties of genetic rescue. Trends Ecol Evol. 2019:34:1070–1079.

Bijlsma R, Westerhof MDD, Roekx LP, Pen I. Dynamics of genetic rescue in inbred *Drosophila melanogaster* populations. Conserv Genet. 2010:11:449–462.

Castellano S, Parra G, Sánchez-Quinto FA, Racimo F, Kuhlwilm M, Kircher M, Sawyer S, Fu Q, Heinze A, Nickel B, et al. Patterns of coding variation in the complete exomes of three Neandertals. Proc Natl Acad Sci USA. 2014:111:6666–6671.

Edmands S. Between a rock and a hard place: evaluating the relative risks of inbreeding and outbreeding for conservation and management. Mol Ecol. 2007:16:463–475.

Eyre-Walker A, Woolfit M, Phelps T. The distribution of fitness effects of new deleterious amino acid mutations in humans. Genetics. 2006:173:891–900.

Fitzpatrick SW, Bradburd GS, Kremer CT, Salerno PE, Angeloni LM, Funk WC. Genomic and fitness consequences of genetic rescue in wild populations. Curr Biol. 2020:30:517–522.e5.

Fitzpatrick SW, Gerberich JC, Angeloni LM, Bailey LL, Broder ED, Torres-Dowdall J, Handelsman CA, López-Sepulcre A, Reznick DN, Ghalambor CK, et al. Gene flow from an adaptively divergent source causes rescue through genetic and demographic factors in two wild populations of Trinidadian guppies. Evol Appl. 2016:9:879–891.

Frankham R. Genetic rescue of small inbred populations: meta-analysis reveals large and consistent benefits of gene flow. Mol Ecol. 2015:24:2610–2618.

Frankham R. Genetic rescue benefits persist to at least the F3 generation, based on a meta-analysis. Biol Conserv. 2016:195:33–36.

Frankham R, Ballou JD, Eldridge MDB, Lacy RC, Ralls K, Dudash MR, Fenster CB. Predicting the probability of outbreeding depression. Conserv Biol. 2011:25:465–475.

Gharrett AJ, Smoker WW, Reisenbichler RR, Taylor SG. Outbreeding depression in hybrids between odd-and even-broodyear pink salmon. Aquaculture. 1999:173:117–129.

Haller BC, Messer PW. SLiM 3: forward genetic simulations beyond the wright–fisher model. Mol Biol Evol. 2019:36:632–637.

Harris K, Nielsen R. The genetic cost of Neanderthal introgression. Genetics. 2016:203:881–891.

Harris K, Zhang Y, Nielsen R. Genetic rescue and the maintenance of native ancestry. Conserv Genet. 2019:20:59–64.

Hayward LK, Sella G. Polygenic adaptation after a sudden change in environment. Elife. 2022:11:e66697.

Heber S, Varsani A, Kuhn S, Girg A, Kempenaers B, Briskie J. The genetic rescue of two bottlenecked South Island robin populations using translocations of inbred donors. Proc Biol Sci. 2012:280:20122228.

Hedrick PW, Fredrickson R. Genetic rescue guidelines with examples from Mexican wolves and Florida panthers. Conserv Genetics. 2009:11:615–626.

Hedrick PW, Garciadorado A. Understanding inbreeding depression, purging, and genetic rescue. Trends Ecol Evol. 2016:31:940–952.

Hedrick PW, Hellsten U, Grattapaglia D. Examining the cause of high inbreeding depression: analysis of whole-genome sequence data in 28 selfed progeny of Eucalyptus grandis. New Phytol. 2016:209:600–611.

Hedrick PW, Robinson JA, Peterson RO, Vucetich JA. Genetics and extinction and the example of Isle Royale wolves. Anim Conserv. 2019:22:302–309.

Hogg JT, Forbes SH, Steele BM, Luikart G. Genetic rescue of an insular population of large mammals. Proc Biol Sci. 2006:273:1491–1499.

Holmes GD, James EA, Hoffmann AA. Limitations to reproductive output and genetic rescue in populations of the rare shrub *Grevillea repens* (Proteaceae). Ann Bot (Lond). 2008:102:1031–1041.

Hwang AS, Northrup SL, Peterson DL, Kim Y, Edmands S. Long-term experimental hybrid swarms between nearly incompatible *Tigriopus californicus* populations: persistent fitness problems and assimilation by the superior population. Conserv Genet. 2012:13:567–579.

Johnson WE, Onorato DP, Roelke ME, Land ED, Cunningham MW, Belden RC, McBride R, Jansen D, Lotz M, Shindle D, et al. Genetic restoration of the Florida Panther. Science. 2010:329:1641–1645.

Jørgensen DB, Ørsted M, Kristensen TN. Sustained positive consequences of genetic rescue of fitness and behavioural traits in inbred populations of *Drosophila melanogaster*. J Evol Biol. 2022:35:868–878.

Kim BY, Huber CD, Lohmueller KE. Deleterious variation shapes the genomic landscape of introgression. PLoS Genet. 2018:14:e1007741.

Kyriazis CC, Wayne RK, Lohmueller KE. Strongly deleterious mutations are a primary determinant of extinction risk due to inbreeding depression. Evol Lett. 2021:5:33–47.

Lohmueller KE, Albrechtsen A, Li Y, Kim SY, Korneliussen T, Vinckenbosch N, Tian G, Huerta-Sanchez E, Feder AF, Grarup N, et al. Natural selection affects multiple aspects of genetic variation

at putatively neutral sites across the human genome. PLoS Genet. 2011:7:e1002326.
Madsen T, Shine R, Olsson M, Wittzell H. Restoration of an inbred adder population. Nature. 1999:402:34–35.
Miller SM, Druce DJ, Dalton DL, Harper CK, Kotze A, Packer C, Slotow R, Bloomer P. Genetic rescue of an isolated African lion population. Conserv Genetics. 2020:21:41–53.
Prufer K, Racimo F, Patterson N, Jay F, Sankararaman S, Sawyer S, Heinze A, Renaud G, Sudmant PH, De Filippo C, et al. The complete genome sequence of a Neanderthal from the Altai Mountains. Nature. 2014:505:43–49.
Rhymer JM, Simberloff D. Extinction by hybridization and introgression. Annu Rev Ecol Syst. 1996:27:83–109.
Robinson JA, Ortega-Del Vecchyo D, Fan Z, Kim BY, vonHoldt BM, Marsden CD, Lohmueller KE, Wayne RK. Genomic flatlining in the endangered island fox. Curr Biol. 2016:26:1183–1189.
Scally A, Durbin R. Revising the human mutation rate: implications for understanding human evolution. Nat Rev Genet. 2012:13:745–753.
Simons YB, Bullaughey K, Hudson RR, Sella G. A population genetic interpretation of GWAS findings for human quantitative traits. PLoS Biol. 2018:16:e2002985.
Smyser TJ, Johnson SA, Page LK, Hudson CM, Rhodes EJ. Use of experimental translocations of Allegheny woodrat to decipher causal agents of decline. Conserv Biol. 2013:27:752–762.
Tallmon DA, Luikart G, Waples RS. The alluring simplicity and complex reality of genetic rescue. Trends Ecol Evol. 2004:19:489–496.
Whiteley AR, Fitzpatrick SW, Funk WC, Tallmon DA. Genetic rescue to the rescue. Trends Ecol Evol. 2015:30:42–49.
Xue Y, Prado-Martinez J, Sudmant PH, Narasimhan V, Ayub Q, Szpak M, Frandsen P, Chen Y, Yngvadottir B, Cooper DN, et al. Mountain gorilla genomes reveal the impact of long-term population decline and inbreeding. Science. 2015:348:242–224.